

# GENERATION AND ACCELERATION OF UNIFORMLY-FILLED ELLIPSOIDAL BUNCHES OBTAINED VIA SPACE-CHARGE EXPANSION FROM A SEMICONDUCTOR PHOTOCATHODE

P. Piot<sup>1,2</sup>, Y.-E Sun<sup>2</sup>, T. Maxwell<sup>1,2</sup>, J. Ruan<sup>2</sup>, E. Secchi<sup>2\*</sup>, J. C. T. Thangaraj<sup>2</sup>

<sup>1</sup> Department of Physics and Northern Illinois Center for Accelerator &

Detector Development, Northern Illinois University DeKalb, IL 60115, USA

<sup>2</sup> Accelerator Physics Center, Fermi National Accelerator Laboratory, Batavia, IL 60510, USA

## Abstract

We report on the experimental generation, acceleration and characterization of a uniformly-filled electron bunch obtained via space-charge-driven expansion (so called “blow-out regime”) at the A0 photoinjector of Fermilab. The beam is photoemitted from a Cesium-Telluride semiconductor photocathode using a short ( $< 200$  fs) ultraviolet laser pulse. The produced electron bunches are characterized with conventional diagnostics and signature of their ellipsoidal character is observed.

## INTRODUCTION

Three-dimensional uniformly-filled ellipsoidal charge distributions produce space charge fields that have a linear dependence on position within the distribution. The resulting density distributions are therefore immune to space-charge-induced dilution. Besides mitigating emittance dilution, these ellipsoidal bunches are especially less prone to halo formation thereby making these distributions attractive for high-power free-electron lasers. Schemes to generate such distributions using photo-emission electron sources were proposed by Serafini [1] and more recently refined by Luiten *et al.* [2]. The latter proposal uses an ultrashort laser impinging on a prompt photo-emitter in a strong accelerating E-field  $E_0$ . The operating parameters of the electron source are chosen such that the distribution evolution is dominated by linear space charge force. This space-charge-dominated expansion, also re-

ferred to as “blow-out regime”, is achieved when the condition  $(eE_0c\tau_l)/(mc^2) \ll \sigma_0/(\epsilon_0E_0) \ll 1$  is met. Here  $\tau_l$ ,  $c$ ,  $\epsilon_0$ ,  $m$  and  $e$  are respectively the duration of the photoemission process, the speed of light, the vacuum electric permittivity, and the electron mass and charge. The parameter  $\sigma_0 \equiv Q/(\pi r^2)$  is the charge density ( $Q$  is the bunch charge and  $r$  the radius of the laser on the photocathode).

Considering the Fermilab’s A0 photoinjector (A0PI) nominal operating parameters  $E_0 = 35$  MV/m, the conditions for ellipsoidal bunch generation using the blow-out regime can in principle be realized with  $\tau_l = 50$  fs; see Fig. 1 (a). A longer pulse length  $\tau_l = 200$  fs can still support the scheme; see Fig. 1 (b). However, further increasing of  $\tau_l$  eventually is constrained because the values of  $E_0$  has to be decreased as well as the charge densities, in order to meet the “blow-out” condition. The resulting operating points might not be of interest to applications demanding significant (sub-nC) charge per bunch, e.g. high-average-power free-electron lasers.

For prompt-emission photocathodes,  $\tau_l$  is comparable to the laser pulse duration and the formation of ellipsoidal bunches was experimentally confirmed [3, 4]. For semiconductor photocathodes, the slower emission time might affect the production of ellipsoidal bunches via the blow-out regime. To date, there has been no investigation regarding the compatibility of the blow-out regime with semiconductor photocathodes [5, 6]. Such an investigation is the main purpose of this Paper.

## THE A0 PHOTOINJECTOR SETUP

The investigation of ellipsoidal bunches production from a semiconductor photocathode and their subsequent acceleration to  $\sim 16$  MeV was carried at A0PI; see Fig. 2 [7]. In brief, electron bunches are generated via photoemission from a cesium telluride ( $\text{Cs}_2\text{Te}$ ) photocathode located on the back plate of a 1+1/2 cell radio-frequency (rf) cavity operating at 1.3 GHz (the “rf gun”). The rf gun is surrounded by three solenoidal lenses that control the beam’s transverse size and emittance. The beam is then accelerated in a 1.3 GHz superconducting rf cavity. Downstream of the booster cavity, the beam line includes a set of quadrupoles, steering dipoles, and diagnostics stations. The transverse density diagnostics are based on Cerium-doped Yttrium Aluminum Garnet (Ce:YAG) screens (labeled to as “X” in

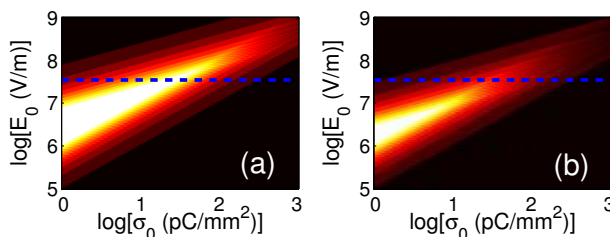


Figure 1: Domain of existence of the blow-out regime (lighter colors) in the  $(\sigma_0, E_0)$  parameter space for  $\tau_l = 50$  fs (a) and  $\tau_l = 200$  fs (b). The horizontal blue dashed lines correspond to  $E_0 = 35$  MV/m.

\* visiting scientist from Politecnico di Milano, Milan, Italy

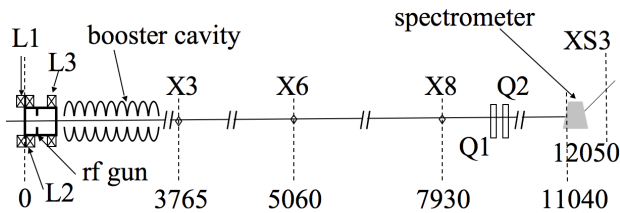


Figure 2: Top view of the AOPi setup displaying elements pertinent to the present simulations and experiments. The “L” refers to solenoidal lenses, “X” to diagnostic stations (beam viewers and/or multi-slit masks location), and “Q” to quadrupole magnets. The distances are in mm and referenced to the photocathode surface.

Fig. 2). A multislit mask insertable at X3 can be used to measure the transverse emittance by analyzing the resulting beamlet’s distribution at the X6 screen [8]. At the end, the beamline incorporates an horizontally-bending spectrometer equipped with a Ce:YAG screen (labeled XS3 in Fig. 2) for energy measurement. The horizontal dispersion value at XS3 location is  $|\eta| = 317$  mm. The nominal operating parameters of the AOPi subsystems are gathered in Table 1.

Nominally, the AOPi’s photocathode laser consists of a frequency-quadrupled Nd:YLF laser. Due to its narrow bandwidth ( $\Delta\lambda \sim 1$  Å), this laser system cannot produce laser pulses with duration  $< 3$  ps. Therefore a short-pulse laser based on a Titanium-Sapphire oscillator and regenerative amplifier was installed. The system also includes an acousto-optic programmable dispersive filter system to control the laser shape. The generated 3-mJ infrared (IR) pulses ( $\lambda = 800$  nm) with duration of  $\sim 50$  fs (rms) are frequency-trippled using two  $\beta$ -BBO crystals of 300 and 150  $\mu$ m thicknesses yielding  $\sim 300$   $\mu$ J ultraviolet (UV) pulses. The frequency conversion scheme was optimized to preserve the short pulse duration using a customized version of SNLO [9]. The estimated duration of the UV pulse is below  $\sim 200$  fs at the photocathode (after transport through a 20-m long optical beamline and passage through three vacuum windows) – a UV frequency-resolved optical gating system is currently being commissioned to precisely measure the UV pulse duration.

## NUMERICAL SIMULATIONS

To confirm whether the AOPi facility could support the production of ellipsoidal bunch using the “blow-out” regime, particle-in-cell simulations were performed using ASTRA [10]. The initial conditions for the electron beam generation are given by the photocathode drive-laser. For the present simulation, the UV laser was assumed to be a Gaussian pulse with 50 fs (rms) duration. However, contrary to metallic photocathodes, their semiconductor counterparts have a finite emission time generally described as a diffusion process. Measurement performed for NEA

cathode have validated this model and response time in the ps regime were reported [11, 12]. To our knowledge there is no corresponding data for Cs<sub>2</sub>Te cathodes and to date the response time were only investigated numerically via Monte-Carlo simulations of the three-step model [13].

These numerical results indicate a significant spread in

Table 1: Nominal settings for the rf-gun, booster cavity, and the photocathode UV laser.

parameter	value	units
laser injection phase <sup>a</sup>	$45 \pm 5$	rf deg
laser radius on cathode	[0.3,2]	mm
laser rms pulse duration	$< 200$	fs
bunch charge	[100~700]	pC
$E_z$ on cathode	$33.7 \pm 0.2$	MV/m
peak $B_z$ <sup>b</sup> (L2, L3)	(0.158~0.041)	T
booster cavity acc. field	$\sim 12.0$	MV/m
booster cavity phase <sup>c</sup>	[-60~60]	rf deg

<sup>a</sup> the phase is referenced w.r.t the zero-crossing phase,

<sup>b</sup> the peak field of solenoid L1 was tuned to zero the axial magnetic field on the photocathode,

<sup>c</sup> the phase is referenced w.r.t. the maximum energy.

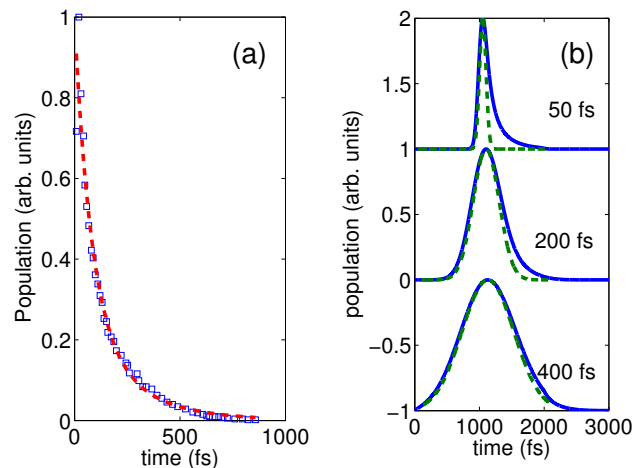


Figure 3: Monte-Carlo simulation (squares) taken from Ref. [13] and parametrization (dashed line) of the electron transit time from an initial Dirac-like laser excitation (a). Impact of the slow response time on the photoemission profile (blue traces) for three different Gaussian-like laser profiles (green dashed traces) of indicated rms duration (b).

electron transit time for an initial Dirac-like laser excitation; see Fig. 3 (a). In particular it is found that 90% of the electrons are emitted within a temporal window of 370 fs. To take into account this finite emission time in our simulation we parametrized the data shown in Fig. 3 (a) with the function  $\Lambda(t)$ . The temporal charge distribution during the photoemission process (at the photocathode surface) is then taken as the convolution  $Q(t) = \int_{-\infty}^{+\infty} Q_0(t')\Lambda(t-t')dt'$

where  $Q_0(t)$  is a Gaussian charge distribution with duration given by the drive laser duration. The results of such a convolution appear in Fig. 3 (b) and show that for laser pulse duration  $\sigma_t \leq 400$  fs, the finite emission of Cs<sub>2</sub>Te significantly alters the profile of the charge emission as it especially leads to an asymmetric distribution with a tail. The

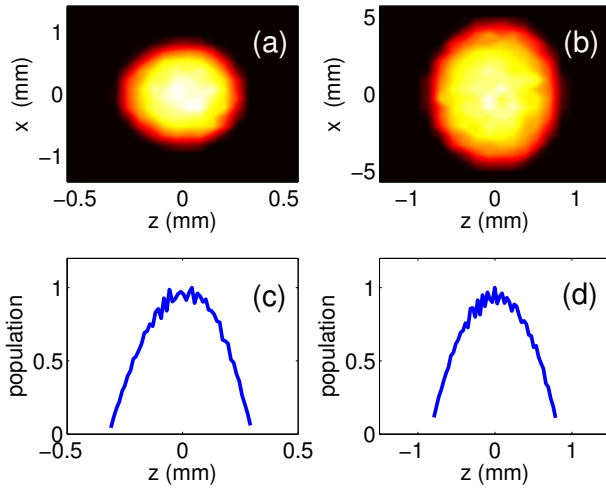


Figure 4: Simulated spatio-temporal distribution ( $z, x$ ) at  $s = 0.47$  m (a) and  $s = 3.77$  m (b) (corresponding to X3 screen) wrt to the photocathode and associated longitudinal charge distributions [(c) and (d) respectively]. The charge is 50 pC and the rms laser transverse size is  $\sigma_c = 1$  mm. In these plots the tail of the bunch is at  $z > 0$ .

finite response time of Cs<sub>2</sub>Te cathode was incorporated in the ASTRA simulations. The transverse distribution of the laser was taken as a  $2\sigma$ -clipped Gaussian distribution. An example of simulated spatio-temporal ( $z, x$ ) densities and associated longitudinal charge distributions appear in Fig. 4 for a charge of  $Q = 50$  pC. The simulations show that for low-charge bunches, the A0PI can support the production of ellipsoidal bunches. Increasing the charge to higher value does not significantly affect the blow-out regime; see Fig. 5.

## EXPERIMENTAL RESULTS

Several experiments were performed to explore the operation of the A0PI in the blow-out regime.

First, we measured the spatio-temporal distribution and explored whether the longitudinal (temporal) profile is described by a parabolic function. For this purpose, we imparted a chirp on the bunch by operating the booster cavity off-crest. The imparted chirp was chosen to have the same sign as the longitudinal phase space chirp. Given the initial longitudinal phase space coordinate of an electron ( $z_0, \delta_0$ ), the final relative momentum spread given by  $\delta_f = A\delta_0 + Bz_0$  where  $A \equiv (E_0/E_f)$  ( $E_0$  and  $E_f$  are respectively the beam's energy upstream and downstream of the booster cavity) and  $B \equiv \frac{-eV_b k \sin \varphi}{E_0 + eV_b \cos \varphi}$  ( $V_b$  is the acceler-

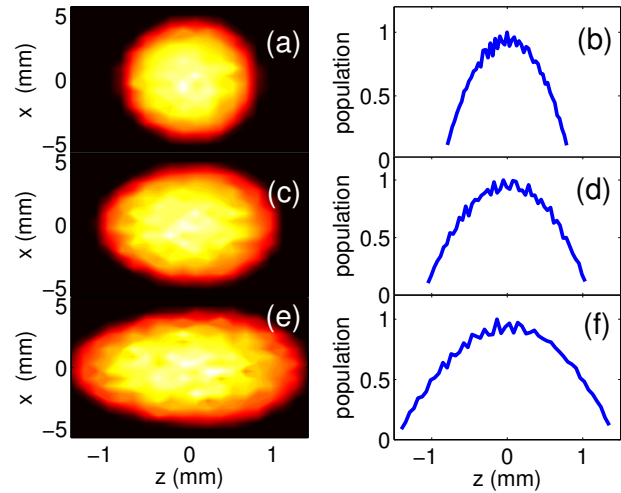


Figure 5: Simulated spatio-temporal distribution ( $z, x$ ) (left column) and associated longitudinal charge distribution (right column) simulated at X3 ( $s = 3.77$  m) for three cases of charges 50 [(a), (b)], 100 [(c), (d)], and 200 pC [(e), (f)]. In these plots the tail of the bunch is at  $z > 0$ .

ating voltage associated to the booster cavity and  $k \equiv 2\pi/\lambda$  with  $\lambda \simeq 0.23$  cm. The latter equation is valid for large off-crest phases, i.e., provided  $\tan \varphi \gg k\sigma_{z,0}$  where  $\sigma_{z,0}$  is the incoming bunch length. Therefore, downstream of the horizontally-bending spectrometer (at XS3), an electron horizontal position is given by

$$x_d = R_{11}x_f + R_{12}x'_f + \eta A\delta_0 + \eta Bz_0, \quad (1)$$

where  $R_{ij}$  stands for the transfer matrix elements from the cavity exit to XS3. By properly tuning the quadrupoles Q1 and Q2, the horizontal position at XS3 is dominated by the last term, i.e.,  $x_d \propto z_0$  and the transverse ( $x_d, y_d$ ) distribution is representative of the ( $z_0, y_d$ ) spatio-temporal distribution. A beam-based calibration procedure was used to infer correspondence to the temporal coordinate by varying the booster cavity phase and recording the beam's centroid motion at XS3. The typical calibration was 57 pixels/ $^\circ$  = 121 pixel/ps.

Examples of measured spatio-temporal distributions for bunch charges ranging from  $\sim 100$  to  $\sim 700$  pC appear in Fig. 6. At low charges the current profiles follow the expected parabolic distribution. As the charge increases the parabolic character in the bunch tail region [ $(z, t) < 0$ ] get distorted. This distortion stems from the image charge becoming important as the charge is increased. For  $Q = 130$  pC, the measured bunch duration is  $\sim 10$  ps full width [corresponding to  $\sim 10/(2\sqrt{5}) \simeq 3$  ps (rms)]. This final bunch duration represents a 10-fold increase compared to the initial laser rms duration of  $\sim 200$  fs. Such a large expansion is a salient feature of the blow-out regime.

A second set of experiments consisted in measuring the incoming longitudinal phase space chirp by operating the booster cavity with an off-crest phase to minimize

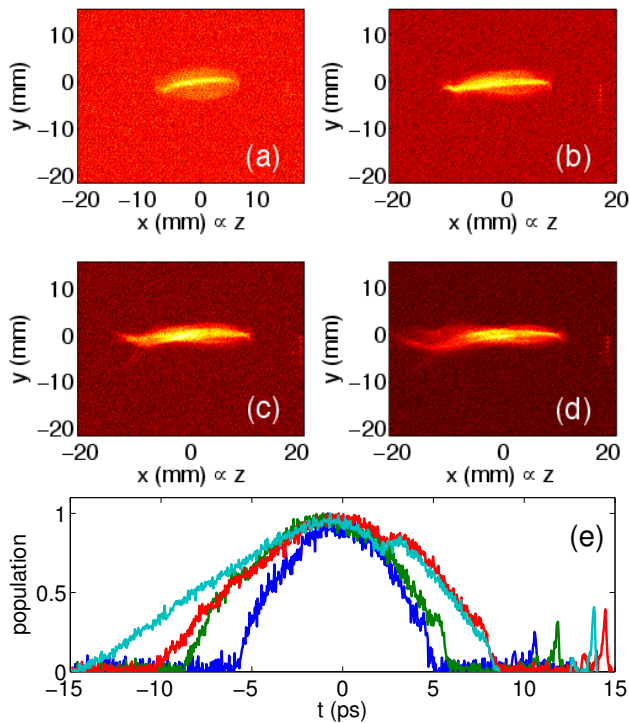


Figure 6: Measured spatio-temporal distribution  $(z, y)$  measured at XS3 for four different charges  $130 \pm 20$  (a),  $280 \pm 20$  (b),  $461 \pm 35$  (c) and  $699 \pm 60$  pC (d) and corresponding normalized current distribution (e) [blue, green, red, cyan traces respectively correspond to images (a), (b), (c) and (d)]. In these plots the tail of the bunch is at  $(z, t) < 0$ .

the momentum spread measured at XS3. As expected for the blow-out regime, the off-crest phase required to minimize the final momentum spread is  $\sim 55^\circ$  which is significantly larger than the phase required for the longer pulses produced with the nominal Nd:YLF laser ( $\sim 25^\circ$ ). Such large off-crest phase is indicative of the strongly correlated longitudinal phase space.

Finally, the transverse emittance of the produced bunches were measured for different laser spot size  $\sigma_c$  and charge  $Q$ . The best emittance measured so far for the minimum charge  $Q = 200 \pm 20$  pC and  $\sigma_c = 1.2 \pm 0.1$  mm was  $1.7 \pm 0.2$   $\mu\text{m}$ .

## SUMMARY

We have demonstrated the production of uniformly-filled ellipsoidal bunch in a L-band rf photoinjector by illuminating a  $\text{Cs}_2\text{Te}$  photocathode with an ultrashort UV pulse. The bunch ellipsoidal character was shown to be preserved after acceleration to  $\sim 16$  MeV.

Further studies are planned at the High-Brightness Electron-beam Source Laboratory (HBESL) which will be commissioned once the AOPi is decommissioned in the Fall 2011. At HBESL, a 3.9-GHz deflecting cavity located

downstream of the rf gun will enable a precise characterization of the longitudinal phase space and possibly the exploration of the response time of  $\text{Cs}_2\text{Te}$  photocathode.

## ACKNOWLEDGMENTS

We are indebted to R. Montiel, J. Santucci, and B. Tennis for their excellent operational and technical supports. We thank M. Church, H. Edwards, E. Harms, A. H. Lumpkin, and V. Shiltsev for their interest and encouragement. One of us (PP) wishes to thank Dr. Smith of AS-Photonics and Dr. Gilevich of SLAC for their help with SNLO. This work supported by the DOD's DURIP award N00014-08-1-1064 to Northern Illinois University and by the DOE contract DE-AC02-07CH11359 to the Fermi Research Alliance LLC.

## REFERENCES

- [1] L. Serafini, in *Advanced Accelerator Concepts* edited by J. S. Wurtele, AIP Conf. Proc. **413** (AIP, New-York), 645 (1993).
- [2] O. J. Luiten, *et al.*, Phys. Rev. Lett. **93**, 094802 (2004).
- [3] P. Musumecchi, *et al.*, Phys. Rev. Lett. **100**, 244801 (2008).
- [4] J. T. Moody, *et al.*, Phys. Rev. ST Accel. Beams **12**, 070704 (2009).
- [5] B. O'Shea, *et al.*, Phys. Rev. ST Accel. Beams **14**, 012801 (2011).
- [6] The recent study reported in Ref. [5] does not use a short laser pulse and cannot explore the possible limitations coming from the  $\text{Cs}_2\text{Te}$  response time. In addition the experimental results reported in Ref. [5] do not provide a clear evidence that the conditions for the blow-out regime were attained.
- [7] J.-P. Carneiro, *et al.*, Phys. Rev. ST Accel. Beams **8**, 040101 (2005).
- [8] A. H. Lumpkin, *et al.*, Phys. Rev. ST Accel. Beams **14**, 060704 (2011).
- [9] SNLO is free software developed by Dr. Arlee Smith and available at <http://www.as-photonics.com/SNLO.html>.
- [10] K. Flöttmann, *ASTRA: A space charge algorithm, User's Manual*, available from the world wide web at <http://www.desy.de/~mpyf10/AstraDokumentation> (unpublished).
- [11] P. Hartmann, *et al.*, J. Appl. Phys. **86**, 2245 (1999).
- [12] I. V. Bazarov, *et al.*, J. Appl. Phys. **103**, 054901 (2008).
- [13] G. Ferrini, *et al.*, Sol. State Comm. **106**, ??? (1998).